Pergamon

Int. J. Solids Structures Vol. 35, No. 16, pp. 2001–2021, 1998

0020–7683/98 $19.00 + .00

PII: S0020–7683(97)00131–5

RE-POLARIZATION OF ELASTIC WAVES AT A FRICTIONAL CONTACT INTERFACE—I. INCIDENCE OF AN SH WAVE

WANG YUE-SHENG
Institute of Engineering Mechanics, Northern Jiaotong University, Beijing 100044, People's Republic of China
E-mail: yswang@center.njtu.edu.cn

YU GUI-LAN

Department of Civil Engineering, Northern Jiaotong University, Beijing 100044, People's Republic of China

and

GAI BING-ZHENG

Department of Astronautics and Mechanics, Harbin Institute of Technology, Harbin 150001, People's Republic of China

(*Received* 10 *February* 1997; *in revised form* 4 *May* 1997)

Abstract—This paper examines the interaction of an incident SH wave with a frictional contact interface between two solids which are pressed together. The incident wave is assumed strong enough to break friction so that localized slip takes place. It is also assumed that the solids are loaded by both anti-plane and in-plane shearing tractions which lead to a global sliding motion. An important and interesting phenomenon is that the incident SH wave is re-polarized at the interface so that the in-plane waves are induced because of the existence of the in-plane shearing traction. The present problem is indeed a nonlinear boundary value problem since the mixed boundary conditions involve unknown intervals (the slip and stick zones). Using Fourier analysis, we manage to reduce the problem to a set of algebraic equations coupled with simple integral equations. An iterative procedure is developed based on the solution to the welded interface. The locations and sizes of the slip zones, the interface shearing tractions, the slip velocities, the global sliding velocity and the energy dissipation and partition are displayed for the case of two identical materials. The present analysis is limited to the sub-critical angle incidence. © 1998 Elsevier Science Ltd.

1. INTRODUCTION

The reflection and refraction of elastic waves at an interface between two solids is of fundamental interest in many fields such as earthquake engineering, geophysics, layered composite materials, civil engineering, etc. This problem is customarily treated on the basis that the interface is welded, meaning that the displacements and stresses are continuous across the interface, or is imperfectly bonded with the interface traction proportional to the displacement jump across the interface. The propagation of elastic waves with these boundary conditions is a linear problem and has been studied extensively. Much less attention has been given to situations in which the two solids are in contact with each other with friction (but no bond). In this case, if the waves are strong enough, the local slip and separation may take place at the interface. Examples of such situations may include the wave propagation in mechanical systems with bolted or press-fit connections and the propagation of seismic waves through a pre-existing fault surface. Precise theoretical modeling of motion and energy transformation in ultrasonic motors, the devices that transform vibrational and wave motions of solids into progressive or rotational motions of rigid bodies by means of frictional forces in contact, may be related to these problems. Zharii (1995, 1996) discussed theoretical modeling of a traveling wave ultrasonic motor.

In the conventional reflection–refraction problem which assumes a perfect bond between two solids or imperfect bond with a linear relation between the traction and the displacement jump, the boundary conditions are in the form of equalities and, therefore, the interface is called a bilateral interface. The associated problem is a bilateral problem. On the contrary, the frictional contact interface with possible slip and separation is termed unilateral interface because the boundary conditions involve inequalities. The corresponding problem is the unilateral problem. The mathematical procedure in the unilateral problem is generally more difficult due to the fact that the boundary conditions are mixed, and that the intervals where the inequalities hold are not known before the solution of the problem. Two analytical methods have been used to study the wave propagation in the presence of the unilateral interface. One is the approximate method used by Miller and Tran, based on equivalent linearization technique. Another is the exact method developed by Comninou and Dundurs. Equivalent linearization technique was presented by Iwan (1973) in a general sense. In this approach the nonlinear term in the governing equations is replaced by a combination of linear terms in such a way that the mean-square difference between the resulting linear and the original nonlinear systems is minimized for all harmonic solutions. Miller (1977) applied this method to the transmission of harmonic SH waves through a frictional interface in the case of normal incidence, and then, with Tran (1979, 1981), to the case of oblique incidence including both anti-plane motion (SH wave) and in-plane motion (P and SV waves). In their analysis, the Coulomb friction model was adopted, and the angle of incidence was assumed to be sub-critical to exclude the total reflection. Moreover, the possible separation was ignored on the basis that the external pressure was sufficiently strong to keep the normal traction at the interface being negative. In another paper, Miller (1978) discussed the effects of various friction models. The propagation of Love-type surface waves in an elastic layer bonded by Coulomb friction to an elastic half-space was also studied by assuming that the attenuation in the system was very small (Miller, 1979).

Comninou and Dundurs developed an exact approach based on the Fourier analysis and the singular integral equation technique and made an extensive investigation on the interaction of elastic waves with a unilateral interface. Their works include: (i) reflection and refraction of harmonic P and SV waves at a smoothly contact interface involving separation for both sub-critical and super-critical angle incidence (Comninou and Dundurs, 1977a, 1977b, 1978a); (ii) reflection and refraction of harmonic P and SV waves at a frictional interface in presence of slip and separation for sub-critical angle incidence (Comninou and Dundurs, 1979a); (iii) transmission of harmonic SH waves through a frictional interface for both sub-critical and super-critical angle incidence (Chez, Dundurs and Comninou, 1978, 1983; Comninou, Dundurs and Chez, 1979); (iv) propagation of interface waves along a smoothly contact interface and a frictionally contact interface (Comninou and Dundurs, 1977c, 1978b); (v) interaction of an elastic pulse with a smoothly or frictionally contact interface (Dundurs and Comninou, 1979; Comninou and Dundurs, 1979b, 1980; Comninou *et al.*, 1982); and (vi) transmission of wave motion between two solids with an initial gap (Barber *et al.*, 1982). With a similar approach, we discussed the frictional slip of an elastic layer with finite thickness on a substrate caused by an SH pulse (Wang *et al.*, 1997). The published results show that the wave propagation in presence of the unilateral interface has many new aspects in physics. For instance, the reflected and refracted waves become distorted in relation to the incident wave and, for an incident harmonic wave, contain higher frequencies. The presence of friction may cause energy dissipation. In this paper we will consider another important feature: the re-polarization of elastic waves at a frictional contact interface.

It is noted that the investigations we mentioned before treated the in-plane and anti-plane wave motion separately. However, if the solids are loaded by in-plane as well as anti-plane shearing traction, an incident SH or P(SV) wave may induce both in-plane and anti-plane motion which are coupled because of the nonlinear boundary conditions. In other words, an incident wave will be re-polarized at a frictional contact interface. As a preliminary analysis, the present paper examines the in-plane wave motion induced by an incident SH wave. The exact method similar to that developed by Comninou and Dundurs

is employed. The mixed boundary conditions lead to a set of algebraic equations coupled with simple integral equations. An iterative procedure is developed to solve these equations. The local slip, the global sliding and the energy partition and dissipation are discussed. The numerical results for the case of frictional contact of two identical materials are presented. The present analysis is limited to the sub-critical angle incidence. It is noted that SH waves do not lead to the separation.

2. PROBLEM FORMULATION

Consider the problem shown in Fig. 1. Two elastic half-spaces are forced together by the applied pressure p_0 and at the same time loaded by the anti-plane shearing traction τ_0 as well as the in-plane shearing traction q_0. With few exceptions the notation we follow is the same as that used by Comninou and Dundurs (1979a). Thus, λ and μ denote the Lamé constant and shear modulus, respectively, and c_L and c_T the velocities of longitudinal and transverse waves. Bars are used to refer to the material constants associated with the upper half space. The Coulomb frictional model between two solids is adopted with static and kinetic friction coefficients as f_s and f_k. Generally, $f_s \geqslant f_k$. An incident harmonic SH wave ($n = 0$) strikes the interface under the angle θ_0, and is reflected and refracted at the interface. If the incident wave is strong enough to break the friction, the in-plane shearing traction may lead to the in-plane motion and ,therefore, induces the P and SV waves in two component materials. The indices $n = 1, 2, 3, 4$, which may appear in suffix or affix positions are to distinguish between the induced P and SV waves, and $n = 2', 4'$ to distinguish between the reflected and refracted SH waves. The coordinate system (x_1, x_2, x_3) is also shown in the figure.

The displacements associated with the different SH waves are taken as the real part of the typical form

$$\mathbf{u}^{(n)} = C_n \mathbf{d}^{(n)} \exp(iy_n), \quad n = 0, 2', 4', \tag{1}$$

where

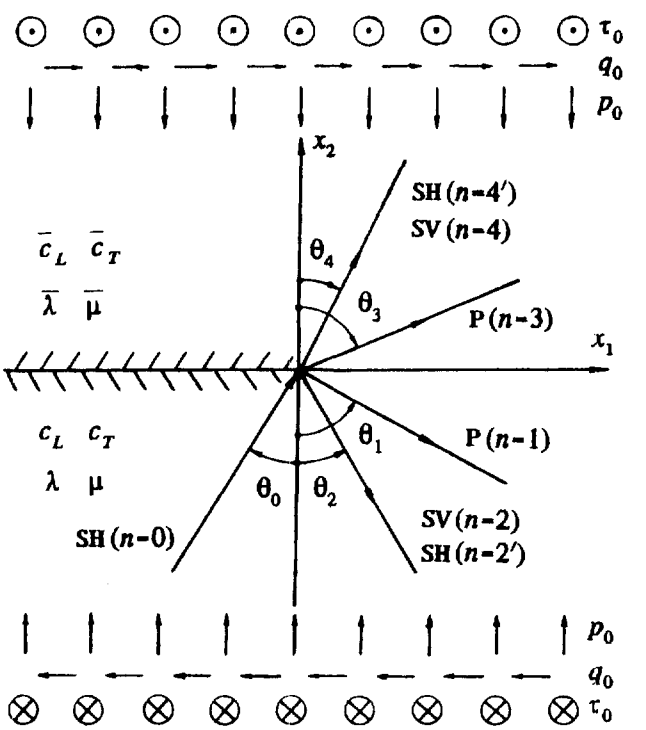

Fig. 1. Interaction of an SH wave with a frictional contact interface.

$$y_n = k_n[\mathbf{x}\cdot\mathbf{p}^{(n)} - c_n t], \tag{2}$$

where k_n denoting the corresponding wave number. $\mathbf{d}^{(n)}$ and $\mathbf{p}^{(n)}$ are, respectively, the unit vectors defining the directions of motions and propagation. They are listed in the Appendix. The amplitude C_n is generally complex. The induced P and SV waves may be taken as the real part of the following form

$$\mathbf{u}^{(n)} = B_n\mathbf{d}^{(n)}\exp(iy_n), \quad n = 1,2,3,4 \tag{3}$$

where y_n is the same as eqn (2), B_n is complex, and the unit vectors $\mathbf{d}^{(n)}$ and $\mathbf{p}^{(n)}$ are given in the Appendix.

To write the boundary conditions, the following displacement, velocity and stress components on $x_2 = 0$ are needed

$$\{u_1^{(n)}, u_2^{(n)}, u_3^{(n)}\} = \{B_n d_1^{(n)}, B_n d_2^{(n)}, C_n\}\exp(i\eta_n) \tag{4}$$

$$\{\dot{u}_1^{(n)}, \dot{u}_2^{(n)}, \dot{u}_3^{(n)}\} = -ik_n c_n\{B_n d_1^{(n)}, B_n d_2^{(n)}, C_n\}\exp(i\eta_n) \tag{5}$$

$$\{\sigma_{12}^{(n)}, \sigma_{22}^{(n)}, \sigma_{23}^{(n)}\} = ik_n\{B_n\mu(d_1^{(n)}p_2^{(n)} + d_2^{(n)}p_1^{(n)}), B_n[\lambda d_1^{(n)}p_1^{(n)} + (\lambda+2\mu)d_2^{(n)}p_2^{(n)}], C_n\mu p_2^{(n)}\}\exp(i\eta_n) \tag{6}$$

where

$$\eta_n = y_n|_{x_2=0} = k_n[x_1 p_1^{(n)} - c_n t]. \tag{7}$$

It was demonstrated that the Snell's law still holds for the unilateral interface (Comninou and Dundurs, 1979a; Chez *et al.*, 1978). Thus we have

$$\eta_0 = \eta_{2'} = \eta_{4'} \triangleq \eta^{\mathrm{SH}}, \quad \eta_1 = \eta_2 = \eta_3 = \eta_4 \triangleq \eta^{\mathrm{PSV}}. \tag{8}$$

Since the P and SV waves are introduced by the SH waves, it is reasonable to assert

$$\eta^{\mathrm{SH}} = \eta^{\mathrm{PSV}} \triangleq \eta. \tag{9}$$

Then it follows from eqns (8) and (9) that $\theta_{2'} = \theta_2$, $\theta_{4'} = \theta_4$, and

$$\frac{\sin\theta_0}{c_{\mathrm{T}}} = \frac{\sin\theta_1}{c_{\mathrm{L}}} = \frac{\sin\theta_2}{c_{\mathrm{T}}} = \frac{\sin\theta_3}{\bar{c}_{\mathrm{L}}} = \frac{\sin\theta_4}{\bar{c}_{\mathrm{T}}}, \tag{10}$$

$$k_0 c_{\mathrm{T}} = k_1 c_{\mathrm{L}} = k_2 c_{\mathrm{T}} = k_3\bar{c}_{\mathrm{L}} = k_4\bar{c}_{\mathrm{T}} = \omega. \tag{11}$$

Since we limit the analysis to the case of sub-critical angle incidence in present paper, θ_0 should satisfy

$$\theta_0 < \theta_{\mathrm{cr}} = \min\{\sin^{-1}(c_{\mathrm{T}}/c_{\mathrm{L}}), \quad \sin^{-1}(c_{\mathrm{T}}/\bar{c}_{\mathrm{L}})\}. \tag{12}$$

Note that η is indeed a moving coordinate along the interface (x_1-axis) at the speed $c_{\mathrm{T}}/\sin\theta_0$. This allows us to formulate the problem in the moving coordinate system (η, x_2, x_3). Furthermore, the periodicity of the problem in η means that only one representative interval, say $-\pi < \eta < \pi$, need to be considered. We denote the normal traction at the interface by $N(\eta)$, the in-plane and anti-plane shearing traction by $S_1(\eta)$ and $S_3(\eta)$, the relative slip velocities in x_1- and x_3-direction by $V_1(\eta)$ and $V_3(\eta)$. Then the unilateral boundary conditions may be written as

$$S_1^2(\eta)+S_3^2(\eta) = [f_k N(\eta)]^2 \tag{13}$$

$$\frac{V_1(\eta)}{S_1(\eta)} = \frac{V_3(\eta)}{S_3(\eta)} \tag{14}$$

in the slip zones, and

$$\sqrt{S_1^2(\eta)+S_3^2(\eta)} < f_s|N(\eta)| \tag{15}$$

$$V_1(\eta) = V_3(\eta) = 0 \tag{16}$$

in the stick zones. It is clear that the boundary conditions are nonlinear and involve inequalities. However, the linearity of the governing equations allow us to construct the solution to the unilateral problem by adding the corrective solution $\{\bar{u}_i, \bar{\sigma}_{ij}\}$ to the results for the welded interface (the bilateral solution) $\{u_i, \sigma_{ij}\}$, as Comninou and Dundurs (1979a) did. Consequently, the interface traction and the relative slip velocities can be expressed as

$$N(\eta) = -p_0+[\bar{\sigma}_{22}^{(1)}+\bar{\sigma}_{22}^{(2)}]_{x_2=0} = -p_0+[\bar{\sigma}_{22}^{(3)}+\bar{\sigma}_{22}^{(4)}]_{x_2=0} \tag{17}$$

$$S_1(\eta) = q_0+[\bar{\sigma}_{12}^{(1)}+\bar{\sigma}_{12}^{(2)}]_{x_2=0} = q_0+[\bar{\sigma}_{12}^{(3)}+\bar{\sigma}_{12}^{(4)}]_{x_2=0} \tag{18}$$

$$S_3(\eta) = \tau_0+[\sigma_{23}+\bar{\sigma}_{23}^{(2')}]_{x_2=0} = \tau_0+[\sigma_{23}+\bar{\sigma}_{23}^{(4')}]_{x_2=0} \tag{19}$$

$$V_1(\eta) = [\dot{\bar{u}}_1^{(3)}+\dot{\bar{u}}_1^{(4)}-\dot{u}_1^{(1)}-\dot{\bar{u}}_1^{(2)}]_{x_2=0} \tag{20}$$

$$V_3(\eta) = [\dot{\bar{u}}_3^{(4')}-\dot{\bar{u}}_3^{(2')}]_{x_2=0}. \tag{21}$$

The bilateral solution for the case of welded interface can be found in any book dealing with elastic waves [for instance Achenbach (1973)]. The shearing traction transmitted by the interface can be obtained by a straightforward calculation

$$[\sigma_{23}]_{x_2=0} = [\sigma_{23}^{(0)}+\sigma_{23}^{(2')}]_{x_2=0} = [\sigma_{23}^{(4')}]_{x_2=0} = Re\{iA_0\exp(i\eta)\}, \tag{22}$$

where

$$A_0 = 2\mu C_0 k_0 b^{-1}\cos\theta_0, \tag{23}$$

with $\Gamma = \bar{\mu}/\mu$, $\gamma_T = c_T/c_T$, and

$$b = 1+\frac{\gamma_T\cos\theta_0}{\Gamma\cos\theta_4}. \tag{24}$$

C_0 in eqn (23) is generally complex, but is taken to be real and positive in this paper.

3. CORRECTIVE SOLUTION

Because of the periodicity of the harmonic incident SH wave, the corrective solution may be expressed as the following Fourier series containing all higher frequencies:

$$\tilde{\mathbf{u}}^{(n)} = \{U_1 t, 0, U_3 t\} + Re\left\{\mathbf{d}^{(n)} \sum_{m=1}^{\infty} F_m^{(n)} \exp(imy_n)\right\}, \quad n = 1, 2(2'), 3, 4(4'), \tag{25}$$

where U_1 and U_3 represent, respectively, the global sliding velocities in x_1- and x_3-direction due to the in-plane and anti-plane shearing traction. $F_m^{(n)}$ is coefficient to be determined and may be written as $F_m^{(n)} = D_m^{(n)} + iE_m^{(n)}$ with $D_m^{(n)}$ and $E_m^{(n)}$ being real. Note that the sum from $m = -1$ to $-\infty$ does not appear in eqn (25) because the waves are assumed to propagate to the right (i.e. $\pi/2 > \theta_0 > 0$).

The requirement that the normal and shearing traction be continuous across the interface leads to the following relations

$$F_m^{(4')} = -\frac{\gamma_T \cos\theta_0}{\Gamma \cos\theta_4} F_m^{(2')} \tag{26}$$

$$F_m^{(3)} = \frac{\gamma_L}{\Gamma \bar{q}} [b_1 F_m^{(1)} - \kappa \sin 2(\theta_2 + \theta_4) F_m^{(2')}] \tag{27}$$

$$F_m^{(4)} = \frac{\gamma_L}{\Gamma \bar{\kappa} \bar{q}} [b_3 F_m^{(1)} + \kappa b_4 F_m^{(2)}]. \tag{28}$$

Moreover, the incident SH wave cannot cause separation, which implies that the normal displacement component is continuous across the interface. Thus, we have

$$F_m^{(2)} = -\frac{\lambda_1 \sin 2\theta_1 + \lambda_2 \kappa^2 \cos 2\theta_2}{\lambda_1 \kappa \cos 2\theta_1 - \lambda_2 \kappa \sin 2\theta_2} F_m^{(1)}. \tag{29}$$

In eqns (26)–(29), $\gamma_L = \bar{c}_L/c_L$, $\kappa = c_L/c_T$, $\bar{\kappa} = \bar{c}_L/\bar{c}_T$, b_j ($j = 1, 3, 4$) and λ_j ($j = 1, 2, 3$) may be found in the literature by Comninou and Dundurs (1979a, eqns (3.5)–(3.9), (4.5)–(4.7)).

By using eqns (25)–(29) the interface tractions and slip velocities given by eqns (17)–(21) can be rewritten as

$$N(\eta) = -p_0 + \mu k_0 \frac{\lambda_1}{\lambda_2} \sum_{m=1}^{\infty} m(I_m \sin m\eta + J_m \cos m\eta) \tag{30}$$

$$S_1(\eta) = q_0 + \mu k_0 \sum_{m=1}^{\infty} m(I_m \sin m\eta + J_m \cos m\eta) \tag{31}$$

$$S_3(\eta) = \tau_0 - A_0 \sin\eta + \mu k_0 \cos\theta_0 \sum_{m=1}^{\infty} m(D_m^{(2')} \sin m\eta + E_m^{(2')} \cos m\eta) \tag{32}$$

$$V_1(\eta) = U_1 - k_0 c_L a \sum_{m=1}^{\infty} m(I_m \sin m\eta + J_m \cos m\eta) \tag{33}$$

$$V_3(\eta) = U_3 - k_0 c_T b \sum_{m=1}^{\infty} m(D_m^{(2')} \sin m\eta + E_m^{(2')} \cos m\eta), \tag{34}$$

where $a = \lambda_1^2/\lambda_2 + \lambda_3$, and

$$\{I_m, J_m\} = -\frac{\lambda_2 q}{\lambda_1 \kappa \cos 2\theta_2 - \lambda_2 \kappa \sin 2\theta_2} \{D_m^{(1)}, E_m^{(1)}\}. \tag{35}$$

From eqns (33) and (34), we have

$$U_1 = \frac{1}{2\pi}\int_{-\pi}^{\pi} V_1(\xi)\,\mathrm{d}\xi, \quad U_3 = \frac{1}{2\pi}\int_{-\pi}^{\pi} V_3(\xi)\,\mathrm{d}\xi \tag{36}$$

$$\{I_m, J_m\} = \frac{-1}{\pi k_0 c_L a m}\int_{-\pi}^{\pi} V_1(\xi)\{\sin m\xi, \cos m\xi\}\,\mathrm{d}\xi \tag{37}$$

$$\{D_m^{(2')}, E_m^{(2')}\} = \frac{-1}{\pi k_0 c_T b m}\int_{-\pi}^{\pi} V_3(\xi)\{\sin m\xi, \cos m\xi\}\,\mathrm{d}\xi. \tag{38}$$

It follows from eqns (30)–(34) that the interface traction $N(\eta)$, $S_1(\eta)$ and $S_3(\eta)$ may be expressed in terms of the slip velocities

$$N(\eta) = -p_0 + \frac{\lambda_1}{\lambda_2} A_0[\bar{U}_1 - \bar{V}_1(\eta)] \tag{39}$$

$$S_1(\eta) = q_0 + A_0[\bar{U}_1 - \bar{V}_1(\eta)] \tag{40}$$

$$S_3(\eta) = \tau_0 - A_0 \sin\eta + \alpha A_0[\bar{U}_3 - \bar{V}_3(\eta)], \tag{41}$$

where we have denoted $\alpha = a\kappa b^{-1}\cos\theta_0$, and

$$\{\bar{V}_1, \bar{V}_3, \bar{U}_1, \bar{U}_3\} = \frac{\mu A_0^{-1}}{c_L a}\{V_1, V_3, U_1, U_3\}. \tag{42}$$

Substitution of eqns (39)–(41) to the boundary conditions (13)–(16) yields

$$\{q_0/A_0 + [\bar{U}_1 - \bar{V}_1(\eta)]\}^2 + \{\tau_0/A_0 - \sin\eta + \alpha[\bar{U}_3 - \bar{V}_3(\eta)]\}^2 = f_k^2\left\{-p_0/A_0 + \frac{\lambda_1}{\lambda_2}[\bar{U}_1 - \bar{V}_1(\eta)]\right\}^2 \tag{43}$$

$$\bar{V}_1(\eta)/\{q_0/A_0 + [\bar{U}_1 - \bar{V}_1(\eta)]\} = \bar{V}_3(\eta)/\{\tau_0/A_0 - \sin\eta + \alpha[\bar{U}_3 - \bar{V}_3(\eta)]\} \tag{44}$$

in the slip zones, and

$$\bar{V}_1(\eta) = \bar{V}_3(\eta) = 0 \tag{45}$$

in the stick zones. Moreover eqn (36) yields

$$\bar{U}_1 = \frac{1}{2\pi}\int_{-\pi}^{\pi} \bar{V}_1(\eta)\,\mathrm{d}\eta, \quad \bar{U}_3 = \frac{1}{2\pi}\int_{-\pi}^{\pi} \bar{V}_3(\eta)\,\mathrm{d}\eta. \tag{46}$$

If we knew the extent and location of the slip or stock zones, $\bar{V}_1(\eta)$, $\bar{V}_3(\eta)$, $\bar{U}_1$ and $\bar{U}_3$ could be obtained by solving eqns (43)–(46). Unfortunately, both the slip zones and the stick zones are unknown before the solution of the problem. We can, however, try to estimate the possible size and location of the slip zones based on the bilateral problem. The shearing traction at the welded interface with q_0 being ignored has the distribution sketched

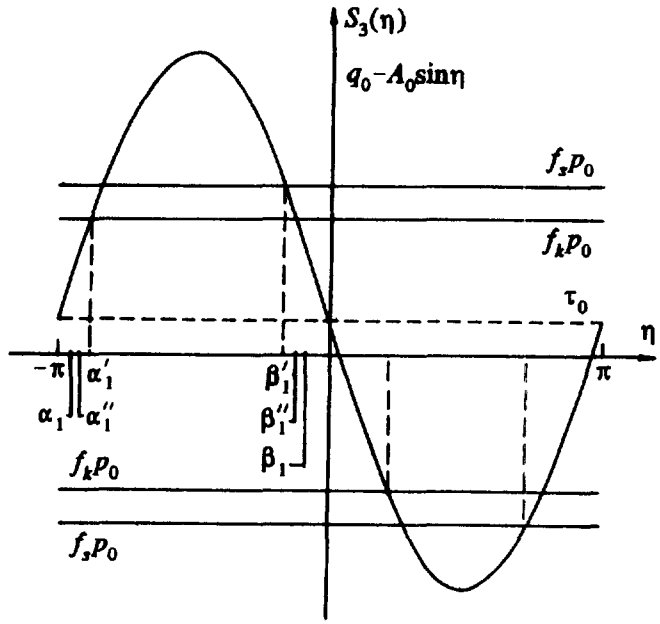

Fig. 2. Anti-plane shearing traction along a welded interface.

in Fig. 2. We think about the bounds $\pm f_s p_0$ and $\pm f_k p_0$ imposed on the shearing traction by the available friction, which are also indicated in the figure. It is clear that, for relative small τ_0, there will be two slip zones in the interval $(-\pi, \pi)$. It is noted that the slip zones propagate to the right (i.e. the positive x_1-direction). Therefore, the shearing traction at the leading edges should reach the level $\pm f_s p_0$ so that slip starts at these edges. Then the shearing traction drops to and keeps at the level $\pm f_k p_0$ in the slip zones until the trailing edges. We suppose that 'slip zones' (note that they are not the real slip zones) takes place where the shearing traction exceeds the friction, as shown in Fig. 2, with (α_1', β_1') denoting the left 'slip zone' centered at $\eta = -\pi/2$ and (α_2', β_2') the right one centered at $\eta = \pi/2$. They are determined by

$$\tau_0/A_0 - \sin\beta_1' = f_s p_0/A_0, \quad \tau_0/A_0 - \sin\beta_2' = -f_s p_0/A_0 \tag{47}$$

$$\tau_0/A_0 - \sin\alpha_1' = f_k p_0/A_0, \quad \tau_0/A_0 - \sin\alpha_2' = -f_k p_0/A_0. \tag{48}$$

Now consider the effect of the applied in-plane shearing traction q_0, which will increase the interface traction to $\sqrt{(\tau_0 - A_0 \sin\eta)^2 + q_0^2}$ with different directions. Thus, the estimated 'slip zones' in presence of q_0, denoted by (α_j'', β_j''), should be larger than the interval (α_j', β_j') and are determined by

$$(\tau_0/A_0 - \sin\beta_j'')^2 + (q_0/A_0) = (f_s p_0/A_0)^2, \quad j = 1, 2 \tag{49}$$

$$(\tau_0/A_0 - \sin\alpha_j'')^2 + (q_0/A_0) = (f_k p_0/A_0)^2, \quad j = 1, 2. \tag{50}$$

The interval (α_j'', β_j'') are certainly not the slip zones which really exist. To determine the real slip zones, one should consider the effects of the corrective solution. Notice that $\bar{V}_1(\eta) = \bar{V}_3(\eta) = 0$ in the stick zones and that λ_1 in practical cases is very small. Then it follows from eqns (39)–(41) that the corrective solution will increase $S_1(\eta)$ and $S_3(\eta)$ in the stick zones with slight influences on $N(\eta)$. As a result, the really existing slip zones, also centered at $\eta = \pm\pi/2$ and denoted by (α_j, β_j), should be larger than the interval (α_j'', β_j'') (this is particularly true when λ_1 is positive). They are determined by

$$(\tau_0/A_0-\sin\beta_j+\alpha\bar{U}_3)^2+(q_0/A_0+\bar{U}_1)^2=f_s^2\left(-p_0/A_0+\frac{\lambda_1}{\lambda_2}\bar{U}_1\right)^2,\quad j=1,2 \tag{51}$$

$$(\tau_0/A_0-\sin\alpha_j+\alpha\bar{U}_3)^2+(q_0/A_0+\bar{U}_1)^2=f_k^2\left(-p_0/A_0+\frac{\lambda_1}{\lambda_2}\bar{U}_1\right)^2,\quad j=1,2. \tag{52}$$

If the applied anti-plane shearing traction τ_0 is sufficiently high, the right slip zone may disappear. Moreover, in some cases the trailing edge α_1 may fall beyond $\eta=-\pi$ and α_2 beyond $\eta=0$. These special situations can be treated individually [cf. Chez *et al.* (1978)].

It should be noted that eqns (51) and (52) cannot yield α_j and β_j, since the unknowns $\{\bar{U}_1, \bar{U}_3\}$ are involved in the equations. That is to say, eqns (51) and (52) are coupled with eqns (43)–(46). A direct approach for solving this equation set may be as follows: first solve eqns (43) and (44) for $\{\bar{V}_1, \bar{V}_3\}$ (whose explicit forms can be obtained since an algebraic equation of four degree is solvable analytically), and eqns (51) and (52) for (α_j, β_j); then substitute them to eqn (46) and solve it for $\{\bar{U}_1, \bar{U}_3\}$. This method is, however, very complex in mathematics, as well as that the explicit solution for $\{\bar{U}_1, \bar{U}_3\}$ cannot be presented. In fact, it is almost impossible to obtain the exact solution of the problem. Thus, to get numerical results, the following iterative procedure may be efficient:

(i) Set $\{\bar{U}_1, \bar{U}_3\}=0$, solve eqns (51) and (52) for (α_j, β_j) and eqns (43) and (44) for $\{\bar{V}_1(\eta), \bar{V}_3(\eta)\}$. Then insert these values into eqn (46) and solve it for $\{\bar{U}_1, \bar{U}_3\}$ which is denoted by $\{\bar{U}_1^{(1)}, \bar{U}_3^{(1)}\}$.

(ii) Substitute $\{\bar{U}_1^{(1)}, \bar{U}_3^{(1)}\}$ to eqns (51), (52), (43) and (44), and solve them for (α_j, β_j) and $\{\bar{V}_1(\eta), \bar{V}_3(\eta)\}$ which are then inserted into eqn (46) to obtain $\{\bar{U}_1, \bar{U}_3\}$ (denoted by $\{\bar{U}_1^{(2)}, \bar{U}_3^{(2)}\}$).

(iii) Repeat step (ii) to obtain $\{\bar{U}_1^{(2)}, \bar{U}_3^{(2)}\}, \ldots, \{\bar{U}_1^{(i)}, \bar{U}_3^{(i)}\}$ until the difference between the result of two nearby interactions is within the expected errors ε, i.e.

$$\max\{|\bar{U}_1^{(i+1)}-\bar{U}_1^{(i)}|, |\bar{U}_3^{(i+1)}-\bar{U}_3^{(i)}|\}\leqslant\varepsilon. \tag{53}$$

It is understood that the initial values of $\{\bar{U}_1, \bar{U}_3\}$ may be selected arbitrarily. However, the selected values close to the real ones can expedite the iteration. Numerical computations for a special case where the two component solids are made of the same materials will be performed in detail afterwards.

4. ENERGY PARTITION AND DISSIPATION

We next examine the power averaged over a wavelength or a period of the incident wave, which is inputted to, extracted from and dissipated at a thin slice of material containing the interface. The power input of the applied in-plane and anti-plane shearing traction is

$$P_q=q_0U_1,\quad P_\tau=\tau_0U_3, \tag{54}$$

whereas the input of the incident wave is

$$P_0=-\frac{1}{2\pi}\int_{-\pi}^{\pi}\sigma_{23}^{(0)}\dot{u}_3^{(0)}\,d\eta=\frac{\mu}{2}C_0^2k_0^2c_T\cos\theta_0. \tag{55}$$

The power extracted from the slice by the reflected SH wave is

$$P_1^{SH} = \frac{1}{2\pi}\int_{-\pi}^{\pi} [\sigma_{23}^{(2')} + \bar{\sigma}_{23}^{(2')}][\dot{u}_3^{(2')} + \dot{\bar{u}}_3^{(2')}]\,d\eta, \tag{56}$$

and that of the refracted SH wave is

$$P_2^{SH} = -\frac{1}{2\pi}\int_{-\pi}^{\pi} [\sigma_{23}^{(4')} + \bar{\sigma}_{23}^{(4')}][\dot{u}_3^{(4')} + \dot{\bar{u}}_3^{(4')}]\,d\eta. \tag{57}$$

While the power extracted by the induced reflected and refracted in-plane waves (P and SV waves) is given by

$$P_1^{PSV} = \frac{1}{2\pi}\int_{-\pi}^{\pi} [\bar{\sigma}_{22}^{(1)} + \bar{\sigma}_{22}^{(2)}][\dot{\bar{u}}_2^{(1)} + \dot{\bar{u}}_2^{(2)}]\,d\eta + \frac{1}{2\pi}\int_{-\pi}^{\pi} [\bar{\sigma}_{12}^{(1)} + \bar{\sigma}_{12}^{(2)}][\dot{\bar{u}}_1^{(1)} + \dot{\bar{u}}_1^{(2)}]\,d\eta \tag{58}$$

$$P_2^{PSV} = -\frac{1}{2\pi}\int_{-\pi}^{\pi} [\bar{\sigma}_{22}^{(3)} + \bar{\sigma}_{22}^{(4)}][\dot{\bar{u}}_2^{(3)} + \dot{\bar{u}}_2^{(4)}]\,d\eta - \frac{1}{2\pi}\int_{-\pi}^{\pi} [\bar{\sigma}_{12}^{(3)} + \bar{\sigma}_{12}^{(4)}][\dot{\bar{u}}_1^{(3)} + \dot{\bar{u}}_1^{(4)}]\,d\eta. \tag{59}$$

The power dissipated by friction at the interface can be divided into two parts. One is due to slip in x_1-direction caused by the interface shearing traction $S_1(\eta)$, which is

$$P_{d1} = \frac{1}{2\pi}\int_{-\pi}^{\pi} S_1(\eta) V_1(\eta)\,d\eta. \tag{60}$$

Another is due to slip in x_3-direction caused by $S_3(\eta)$, which is given by

$$P_{d3} = \frac{1}{2\pi}\int_{-\pi}^{\pi} S_3(\eta) V_3(\eta)\,d\eta. \tag{61}$$

It follows from the energy conservation that

$$P_0 + P_q + P_\tau = P_1^{SH} + P_2^{SH} + P_1^{PSV} + P_2^{PSV} + P_{d1} + P_{d3}, \tag{62}$$

which can be used as a check on the numerical computations.

5. NUMERICAL EXAMPLE AND DISCUSSION

The results of the previous sections are quite general. Indeed, they are only restricted by the assumption that the incident angle θ_0 does not exceed the critical angle θ_{cr}. In order to carry out computations and to give more explicit exploration to the re-polarization of elastic waves, we will however consider identical materials in this section. Then we have

$$\gamma_T = \gamma_L = \Gamma = 1, \quad \theta_1 = \theta_3, \quad \theta_2 = \theta_4 = \theta_0$$

$$\lambda_1 = 0, \quad \lambda_2 = \frac{2}{q}\cos\theta_1, \quad \lambda_3 = \frac{2\kappa}{q}\cos\theta_0, \quad b = 2, \quad a = \lambda_3$$

$$\alpha = \frac{1}{2}\lambda_3\kappa\cos\theta_0, \quad \kappa = \bar{\kappa} = \sqrt{\frac{2-2\nu}{1-2\nu}},$$

where ν is the Poisson ratio of the materials. It is noted that the induced in-plane wave motion has no effects on the interface normal traction $N(\eta)$ because $\lambda_1 = 0$.

Since the re-polarization of waves are caused by the in-plane shearing traction q_0, we neglect the anti-plane shearing traction τ_0 in calculations for simplicity and assume that $f_s = f_k = f$ (that is, the kinematic locking is ignored). The global sliding in x_3-direction will not take place without τ_0, i.e. $U_3 = 0$. In this case, the following relations must be true

$$\alpha_2 = \pi + \alpha_1, \quad \beta_2 = \pi + \beta_1 \tag{63}$$

$$\{V_1(\eta), V_3(\eta)\} = \{V_1(\eta+\pi), -V_3(\eta+\pi)\} \tag{64}$$

$$\{N(\eta), S_1(\eta), S_3(\eta)\} = \{N(\eta+\pi), S_1(\eta+\pi), -S_3(\eta+\pi)\}, \tag{65}$$

which allow us to calculate V_1 and V_3 in one slip zone, say the left one (α_1, β_1). Then eqn (46) reduces to

$$\bar{U} = \frac{1}{\pi}\int_{\alpha_1}^{\beta_1} \bar{V}_1(\eta)\,\mathrm{d}\eta. \tag{66}$$

Under these assumptions, eqns (51) and (52) yield

$$\beta_1 = -\pi - \alpha_1 = -\arcsin\sqrt{(fp_0/A_0)^2 - (q_0/A_0 + \bar{U}_1)^2} \tag{67}$$

from which we can conclude that the interface is perfectly bonded ($\alpha_1 = \beta_1 = -\pi/2$) when

$$fp_0/A_0 > \sqrt{1 + (q_0/A_0)^2}, \tag{68}$$

and that there is no stick zone along the interface ($\alpha_1 = -\pi, \beta_1 = 0$) when

$$fp_0/A_0 = |q_0/A_0 + \bar{U}_1|. \tag{69}$$

In other words, the local slip and stick appear on the interface alternately when

$$|q_0/A_0 + \bar{U}_1| < fp_0/A_0 < \sqrt{1 + (q_0/A_0)^2}. \tag{70}$$

While the local slip without stick takes place if

$$|q_0/A_0| < fp_0/A_0 < |q_0/A_0 + \bar{U}_1|. \tag{71}$$

It is understood that the collapse slipping will happen when $|q_0| \geqslant fp_0$. The motion when $|q_0| < fp_0 < \sqrt{q_0^2 + A_0^2}$ is indeed the creep slip, that is, one half space slides on the other with speeds distributed inhomogeneously along the whole interface.

Equation (44) gives the expression of $\bar{V}_1(\eta)$ in terms of $\bar{V}_3(\eta)$

$$\bar{V}_1(\eta) = \frac{q_0/A_0 + \bar{U}_1}{-\sin\eta + (1-\alpha)\bar{V}_3(\eta)}\bar{V}_3(\eta), \tag{72}$$

which when substituted into eqn (43) yields a quartic equation

$$\bar{V}_3^4(\eta) + \bar{b}\bar{V}_3^3(\eta) + \bar{c}\bar{V}_3^2(\eta) + \bar{d}\bar{V}_3(\eta) + \bar{e} = 0, \tag{73}$$

with

$$\bar{b} = 2(1-2\alpha)\sin\eta/[\alpha(1-\alpha)]$$

$$\bar{c} = [(6\alpha^2 - 6\alpha + 1)\sin^2\eta - (1-\alpha)^2(fp_0/A_0)^2 + \alpha^2(q_0/A_0 + \bar{U}_1)^2]/[\alpha^2(1-\alpha)^2]$$

$$\bar{d} = 2\sin\eta[(2\alpha-1)\sin^2\eta + (1-\alpha)(fp_0/A_0)^2 + \alpha(q_0/A_0 + \bar{U}_1)^2]/[\alpha^2(1-\alpha)^2]$$

$$\bar{e} = \sin^2\eta[\sin^2\eta - (fp_0/A_0)^2 + (q_0/A_0 + \bar{U}_1)^2]/[\alpha^2(1-\alpha)^2].$$

Equation (73) can be solved analytically by using Ferrari's method (Kern and Kern, 1974). We should look for the real solution, which proves to be the roots of the following quadratic equation

$$\bar{V}_3^2(\eta) + \tilde{b}\bar{V}_3(\eta) + \tilde{c} = 0, \tag{74}$$

where

$$\tilde{b} = \frac{1}{2}(\bar{b} - \sqrt{8y + \bar{b}^2 - 4\bar{c}}), \quad \tilde{c} = y - \frac{\bar{b}y - \bar{d}}{\sqrt{8y + \bar{b}^2 - 4\bar{c}}}$$

and y is any one of the three roots of the cubic equation

$$8y^3 - 4\bar{c}y^2 + (2\bar{b}\bar{d} - 8\bar{e})y + \bar{e}(4\bar{c} - \bar{b}^2) - \bar{d}^2 = 0, \tag{75}$$

which can be solved analytically by using Cardano's method (Kern and Kern, 1974). It can be further demonstrated by the computation that the solution of eqn (73) satisfying the condition $\bar{V}_3(\alpha_1) = \bar{V}_3(\beta_1) = 0$ should be

$$\bar{V}_3(\eta) = \tfrac{1}{2}(-\tilde{b} + \sqrt{\tilde{b}^2 - 4\tilde{c}}). \tag{76}$$

For the case of $\alpha = 1$ (corresponding to the normal incidence) eqn (73) reduces to a quadratic equation of the same form as (74) with the coefficients given by

$$\tilde{b} = 2\sin\eta, \quad \tilde{c} = \sin^2\eta\left[1 - \frac{(fp_0/A_0)^2}{\sin^2\eta + (q_0/A_0 + \bar{U}_1)^2}\right].$$

The desired solution has the same form as eqn (76).

Now we can carry out the computation based on eqns (66), (67), (72) and (76) by the iterative procedure described previously. Note that when condition (71) holds we should take $\{\alpha_1, \beta_1\} = \{-\pi, 0\}$. It can be seen that the solution of the problem depends on the three parameters: q_0/A_0, fp_0/A_0 and α, where $\alpha(\geqslant 1)$ involves the effects of Poisson ratio ν and the incident angle θ_0. Set Poisson ratio $\nu = 0.25$. Then the critical incident angle is

$$\theta_{cr} = \sin^{-1}(1/\kappa) = 35.264^\circ. \tag{77}$$

Thus the incident angle should be restricted in the region between 0 and 35.264°.

We first examine the convergence of the iteration by giving an example with $q_0/A_0 = 0.5$, $fp_0/A_0 = 0.7$ and $\alpha = 1.5$ (i.e. $\theta_0 = 30^\circ$). The integrals in eqn (46) are calculated by using

Table 1. Values of β_1 and $\bar{U}_1$ for each step of iteration ($q_0/A_0 = 0.5, fp_0/A_0 = 0.7, \alpha = 1.5$)

ith iteration	β_1 (deg)	$\bar{U}_1^{(i)}$	$\bar{U}_1^{(i)} - \bar{U}_1^{(i-1)}$	$[\bar{U}_1^{(i)} - \bar{U}_1^{(i-1)}]/\bar{U}_1^{(i)}$
1	−29.334	0.070727	0.070727	1
2	−23.910	0.095291	0.024564	0.25778
3	−21.609	0.105104	0.009813	0.09336
4	−20.605	0.109265	0.004161	0.03808
5	−20.162	0.111074	0.001809	0.01629
6	−19.965	0.111869	0.000795	0.00711
7	−19.878	0.112220	0.000351	0.00313
8	−19.840	0.112376	0.000155	0.00138
9	−19.823	0.112444	0.000069	0.00061
10	−19.815	0.112475	0.000030	0.00027
11	−19.812	0.112488	0.000013	0.00012
12	−19.810	0.112494	0.000006	0.00005

the 120-point trapezoid formula. Table 1 lists the values of β_1 and $\bar{U}_1$ for each step of iteration. It is seen that we can get an accuracy of 1% after six iterations, 0.1% after nine iterations and 0.01% after twelve iterations. In the following calculation, the accuracy is kept at the level of 0.1%.

Figure 3 illustrates the distributions of interface shearing tractions and relative slip velocities in the left half period $(-\pi, 0)$ for $q_0/A_0 = 0.5, fp_0/A_0 = 0.8, \theta_0 = 20°$. The results with $q_0 = 0$ are depicted with the dotted curves. While the dashed lines show the results with the induced in-plane waves being neglected. It is seen that, in the stick zone, the induced waves have no influence on the anti-plane shear stress, but increase the in-plane component. The shearing tractions $S_1(\eta)$ and $S_3(\eta)$ are no longer constant with the resultant traction $\sqrt{S_1^2(\eta) + S_3^2(\eta)}$ in the slip zones remaining at the value of friction fp_0. The estimated slip zones (α_1', β_1'), (α_1'', β_1'') (see Section 3) and the real slip zone (α_1, β_1) are also shown in the figures for comparison. It is likely that the induced waves make the interface slip more easily. The results show that the induced waves have significant influences and cannot be

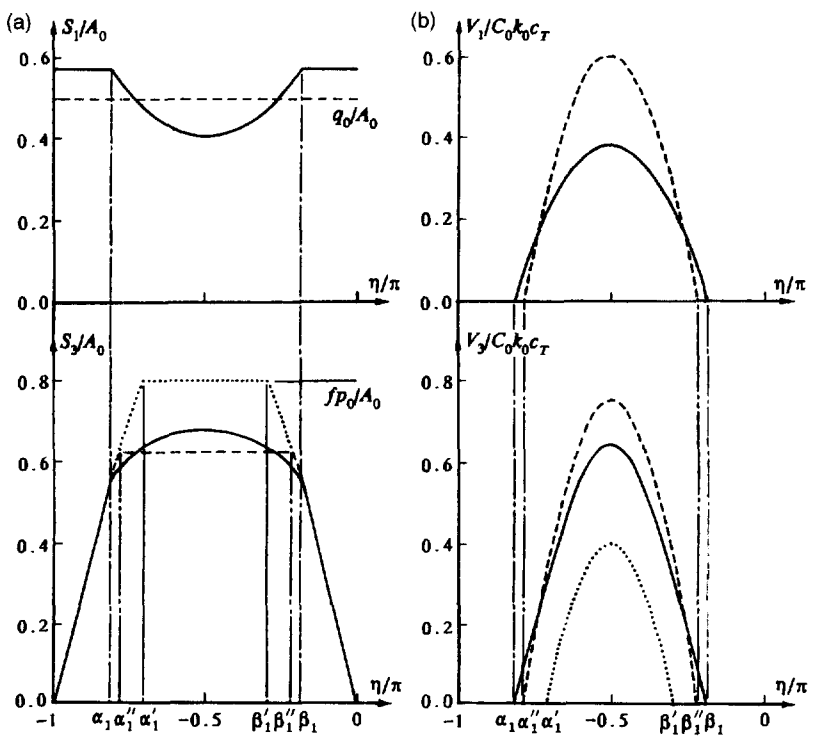

Fig. 3. Distributions of interface shearing tractions (a) and relative slip velocities (b) for $q_0/A_0 = 0.5$, $f_0p_0/A_0 = 0.8$, $\theta_0 = 20°$.

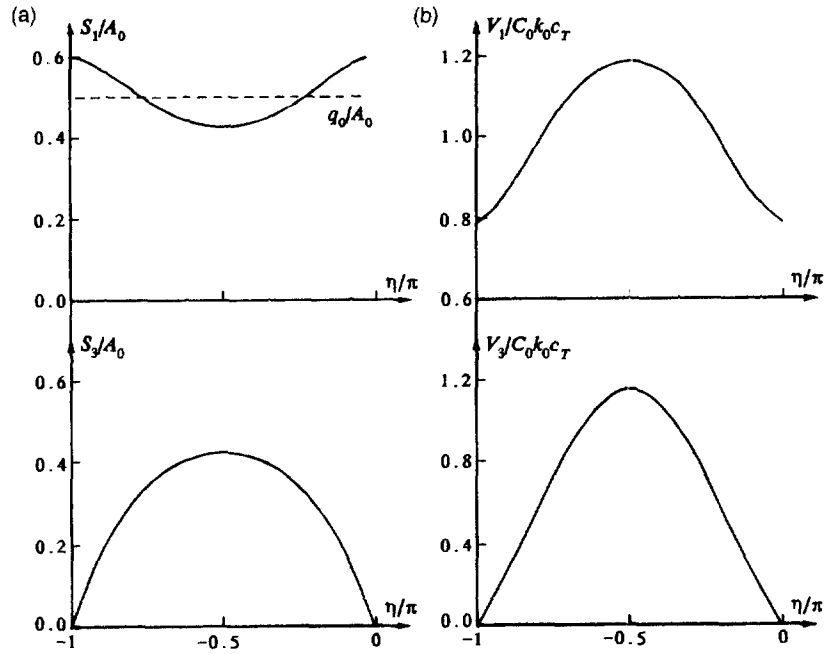

Fig. 4. Distributions of interface shearing tractions (a) and relative slip velocities (b) for $q_0/A_0 = 0.5$, $f_0p_0/A_0 = 0.6$, $\theta_0 = 20°$.

ignored, especially for larger q_0 and/or smaller fp_0. See Fig. 4 which gives the shearing tractions and slip velocities for $q_0/A_0 = 0.5$, $fp_0/A_0 = 0.6$, $\theta_0 = 20°$. In this situation, the interface slips without stick zones. The slip velocities, however, are inhomogeneous along the interface. It is noted that the anti-plane shearing traction $S_3(\eta)$ is smaller and the slip velocities $\{V_1(\eta), V_3(\eta)\}$ are larger in comparison with those shown in Fig. 3. From this fact one can deduce that $S_3(\eta)$ decreases and $\{V_1(\eta), V_3(\eta)\}$ increase with q_0 approaching fp_0. Indeed, one may find the solution in the limiting case of $fp_0 \to q_0$. Equation (43) in this limiting situation yields $\bar{U}_1 = \bar{V}_1(\eta)$ and thus

$$\bar{V}_3(\eta) = -\alpha^{-1} \sin \eta, \tag{78}$$

which implies that the anti-plane shearing traction vanishes at the interface, that is, the interface cannot transmit the anti-plane wave motion in this case. $V_3(\eta)$ given by eqn (78) is exactly the same as the surface particle velocity caused by an incident SH wave in an elastic half space. To satisfy eqn (44), $\bar{U}_1$ and $\bar{V}_1(\eta)$ should be infinitely large. The normalized global sliding velocities (creep velocities) are plotted against fp_0/A_0 in Fig. 5 for different values of q_0/A_0 with $\theta_0 = 20°$. It is shown that the creep velocity increases rapidly to infinity with fp_0 approaching q_0. The incident angle θ_0 has slight effects on the creep velocity as shown in Fig. 6.

Now consider a progressive decrease of fp_0. For a large value of fp_0 satisfying inequality (68), the interface is perfectly bonded (denote this case as Case I). Decrease fp_0 until inequality (70) holds. Then the interface slides with the local slip and stick appearing alternately (Case II). Decrease fp_0 successively to satisfying inequality (71). The stick zones disappear and the relative slip velocities $\{V_1(\eta), V_3(\eta)\}$ increase (Case III). In these two situations, the motion is just like creep. Once fp_0 drops to the level of q_0, the upper half space will slide in a breakdown manner in x_2-direction at an infinitely large speed with respect to the lower half space. No SH wave can be transmitted across the interface and no in-plane wave motion is induced (Case IV). The four cases and the regions they occupy in the fp_0/A_0, q_0/A_0 plane are shown in Fig. 7. The boundary between Case II and III varies with the incident angle θ_0 (or equivalently, α). The figure gives the results for critical-angle incidence, normal incidence and 30°-angle incidence.

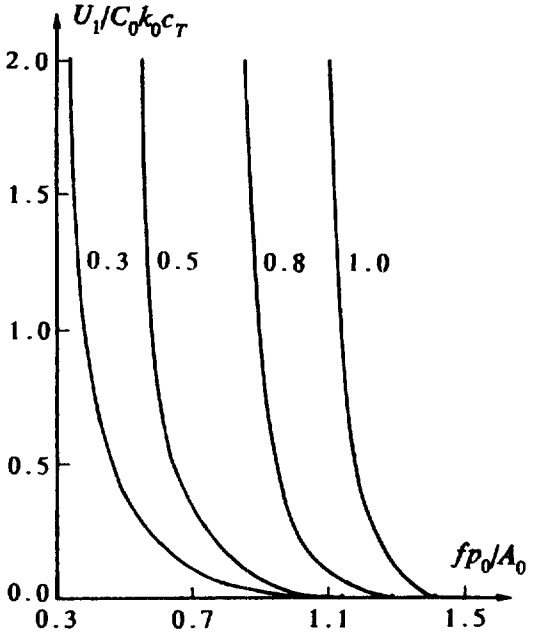

Fig. 5. Dependence of the global sliding (creep) velocity on fp_0/A_0 for some selected values of q_0/A_0 with $\theta_0 = 20^\circ$.

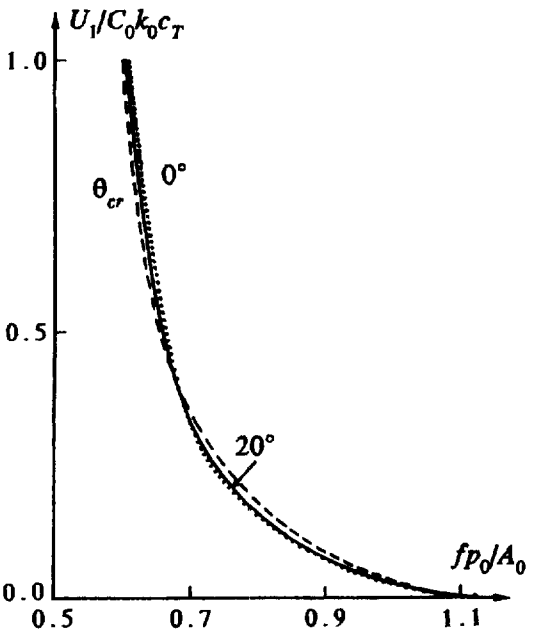

Fig. 6. Effect of the incident angle on the global sliding (creep) velocity, $q_0/A_0 = 0.5$.

Figure 8 presents the curves determining the extent and location of the left slip zone for given fp_0/A_0 and some selected values of q_0/A_0 with $\theta_0 = 20^\circ$. The stronger shearing traction q_0 will lead larger slip zones for a fixed pressure p_0 (with other parameters unchanged). The curve for $q_0/A_0 = 0$, the case discussed by Chez *et al.* (1978), follows exactly the sinusoidal curve. While the curves in presence of q_0 become distorted, especially when the slip zone is large. The effects of the incident angle on the extent and location of slip zones are shown in Fig. 9 for $q_0/A_0 = 0.5$. It is seen that a small-angle incident wave may cause larger local slip zones. However, distinct differences between lines can be observed only when the slip zone is large and the incident angle is very close to critical angle θ_{cr}. This

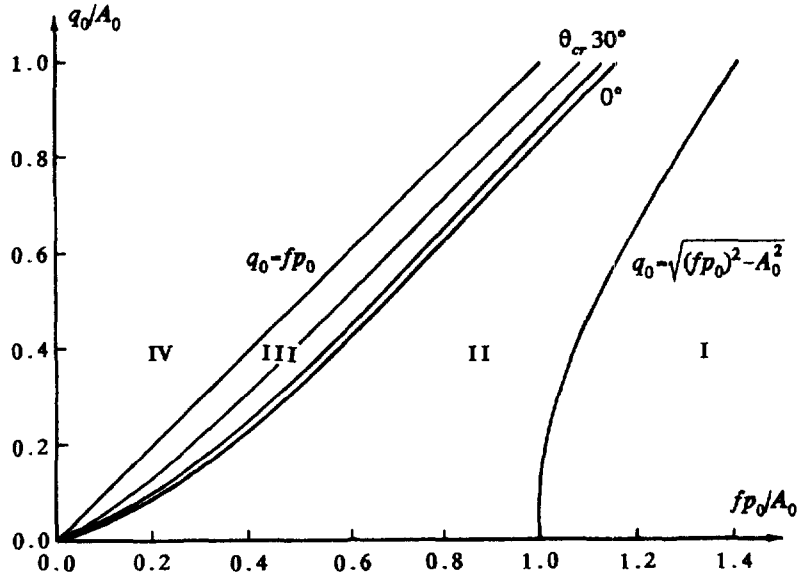

Fig. 7. Classification of four situations for different incident angles ($\theta_0 = 0°, 30°, \theta_{cr}$). Case I—welded interface; Case II—creep slip of the interface in presence of stick zones; Case III—creep slip of the interface without stick zones; Case IV—catastrophic slip of the interface.

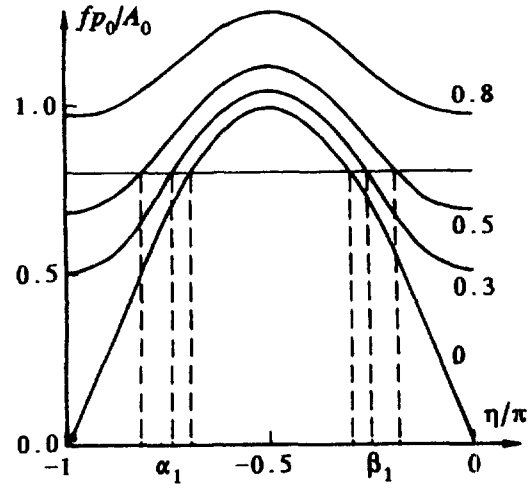

Fig. 8. Extent and location of slip zones for fp_0/A_0 and some selected values of q_0/A_0 with $\theta_0 = 20°$.

is understood by the fact that the parameter α varies slightly for smaller θ_0, but rapidly as θ_0 approaches θ_{cr}.

We next discuss the energy dissipation and partition at the interface. For the particular example considered in this section, a straightforward calculation yields, on the interface,

$$\dot{u}_3^{(2')} = 0, \quad \dot{u}_3^{(4')} = C_0 k_0 c_T \sin\eta$$

$$\sigma_{23}^{(2')} = 0, \quad \sigma_{23}^{(4')} = -A_0 \sin\eta$$

$$\dot{\bar{u}}_3^{(2')} = -\dot{\bar{u}}_3^{(4')} = -\frac{V_3(\eta)}{2}$$

$$\bar{\sigma}_{23}^{(2')} = \bar{\sigma}_{23}^{(4')} = S_3(\eta) + A_0 \sin\eta = -\frac{\mu\cos\theta_0}{2c_T} V_3(\eta)$$

$$\dot{\bar{u}}_1^{(1)} + \dot{\bar{u}}_1^{(2)} = -[\dot{\bar{u}}_1^{(3)} + \dot{\bar{u}}_1^{(4)}] = -\tfrac{1}{2} V_1(\eta)$$

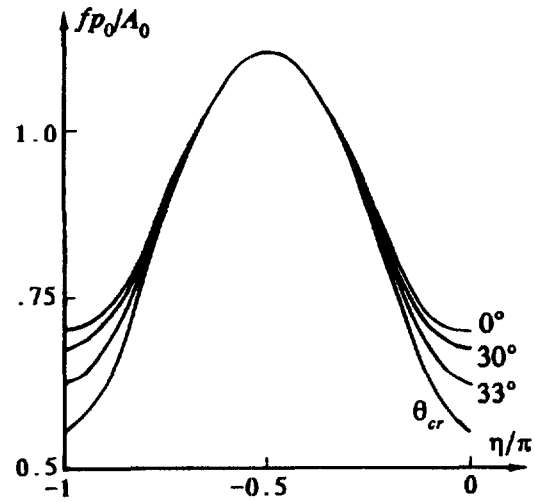

Fig. 9. Effect of the incident angle on the extent and location of slip zones, $q_0/A_0 = 0.5$.

$$\bar{\sigma}_{12}^{(1)} + \bar{\sigma}_{12}^{(2)} = \bar{\sigma}_{12}^{(3)} + \bar{\sigma}_{12}^{(4)} = S_1(\eta) - q_0 = \frac{\mu}{ac_L}[U_1 - V_1(\eta)]$$

$$\bar{\sigma}_{22}^{(1)} + \bar{\sigma}_{22}^{(2)} = \bar{\sigma}_{22}^{(3)} + \bar{\sigma}_{22}^{(4)} = 0.$$

Following the formula in Section 4, we have

$$P_1^{SH} = \frac{1}{2\pi}\int_{-\pi}^{\pi} \frac{\mu \cos\theta_0}{4c_T} V_3^2(\eta)\, d\eta \tag{79}$$

$$P_2^{SH} = \frac{1}{2\pi}\int_{-\pi}^{\pi} \left[A_0 \sin\eta + \frac{\mu\cos\theta_0}{2c_T} V_3(\eta)\right]\left[C_0 k_0 c_T \sin\eta + \frac{V_3(\eta)}{2}\right] d\eta \tag{80}$$

$$P_{d3} = -\frac{1}{2\pi}\int_{-\pi}^{\pi} \left[A_0 \sin\eta + \frac{\mu\cos\theta_0}{2c_T} V_3(\eta)\right] V_3(\eta)\, d\eta \tag{81}$$

$$P_1^{PSV} = P_2^{PSV} = -\frac{1}{2\pi}\int_{-\pi}^{\pi} \frac{\mu}{2\lambda_3 c_T}[U_1 - V_1(\eta)]V_1(\eta)\, d\eta \tag{82}$$

$$P_{d1} = q_0 U_1 + \frac{1}{2\pi}\int_{-\pi}^{\pi} \frac{\mu}{\lambda_3 c_T}[U_1 - V_1(\eta)]V_1(\eta)\, d\eta. \tag{83}$$

It can be verified that

$$P_0 = P_1^{SH} + P_2^{SH} + P_{d3}, \tag{84}$$

which means that the energy input associated with the incident SH wave is converted to the energy carried by the reflected and refracted SH waves and the dissipated energy due to the anti-plane motion of the solids. Similarly, we can find

$$P_q = P_1^{PSV} + P_2^{PSV} + P_{d1}, \tag{85}$$

i.e. part of the energy supplied by the shearing traction q_0 is partitioned equally over the

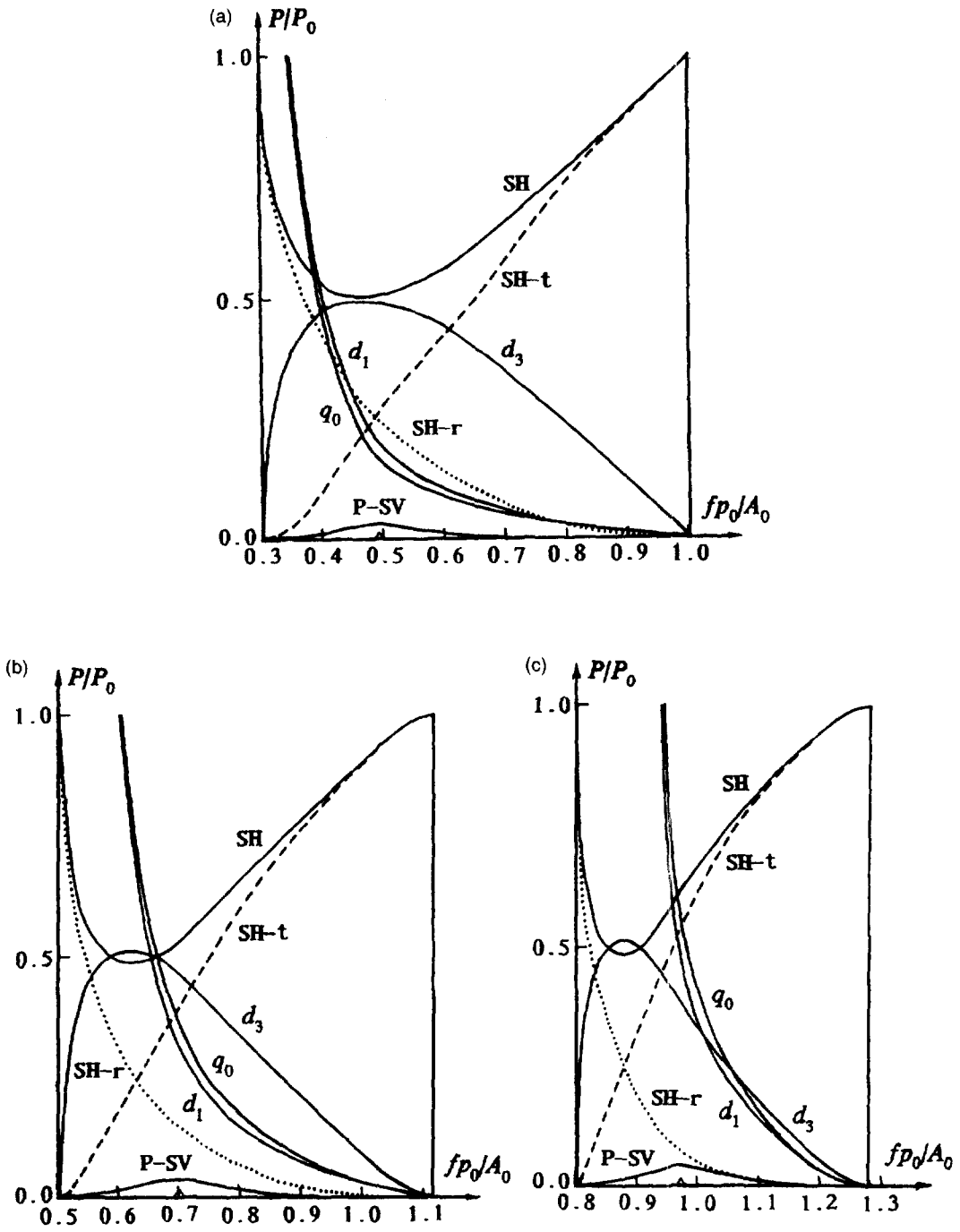

Fig. 10. Energy partition and dissipation for different values of q_0/A_0 with $\theta_0 = 20°$: (a) $q_0/A_0 = 0.3$; (b) $q_0/A_0 = 0.5$; and (c) $q_0/A_0 = 0.8$.

induced reflected and refracted in-plane waves, the rest is dissipated due to the frictional slip in x_1-direction.

The power ratios $\{(P_1^{SH}+P_2^{SH})/P_0, P_{d3}/P_0, P_q/P_0, (P_1^{PSV}+P_2^{PSV})/P_0, P_{d1}/P_0\}$ are plotted vs fp_0/A_0 in Fig. 10 for selected values of q_0/A_0 with $\theta_0 = 20°$. The dashed lines correspond to the refracted SH wave (P_1^{SH}/P_0) and the dotted lines to the reflected one (P_2^{SH}/P_0). The results for normal incidence and critical-angle incidence are presented in Fig. 11 to show the effects of the incident angle θ_0. The power extracted by the induced waves, which reaches a peak value at the moment when stick zones disappear, i.e. when eqn (69) is satisfied (marked by a triangle in the figures), is very small. Most of the power input of q_0 is absorbed by friction. As $fp_0/A_0 \to q_0$, all of the power input P_q is dissipated in P_{d1} and both of them

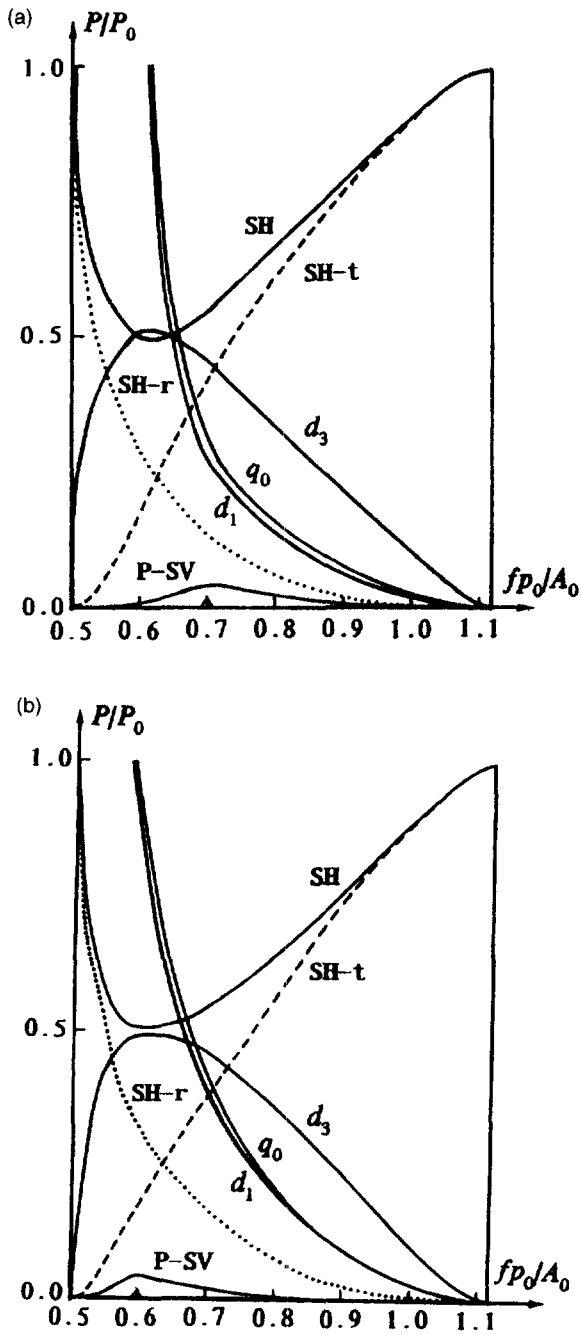

Fig. 11. Energy partition and dissipation for different values of θ_0 with $q_0/A_0 = 0.5$: (a) $\theta_0 = 0°$; and (b) $\theta_0 = \theta_{cr}$.

become infinitely large, which is understood by considering that $U_1 \to \infty$ in this limiting case. Also in this limiting situation, P_2^{SH} and P_{d3} vanish and all of the power input P_0 is transferred to the reflected SH wave (P_1^{SH}). Therefore, when catastrophic slip takes place, the in-plane wave motion cannot be induced and the anti-plane wave motion cannot be transmitted to the upper half space. It is seen from the diagrams that the dissipated power P_{d3} reaches a peak in Case III (see Fig. 7). The peak shifts to the smallest possible value of fp_0/A_0 when q_0/A_0 is increased or when θ_0 approaches the critical angle θ_{cr}.

Although only a specific example is computed and discussed in detail, the method can be extended to other cases without any difficulty. The re-polarization of an incident P or SV wave will be explored in Part II of this series paper by using the similar approach. Possible local separations of the interface will be included in that case.

Acknowledgements—Support by the China National Science Foundation under Grant No. 19472026 is gratefully acknowledged.

REFERENCES

Achenbach, J. D. (1973) *Wave Propagation in Elastic Solids.* North Holland, Amsterdam.

Barber, J. R., Comninou, M. and Dundurs, J. (1982) Contact transmission of wave motion between two solids with an initial gap. *International Journal of Solids and Structures* **18,** 775–781.

Chez, E. L., Dundurs, J. and Comninou, M. (1978). Reflection and refraction of SH waves in presence of slip and friction. *Bulletin of Seismology Society of America* **68,** 999–1011.

Chez, E. L., Dundurs, J. and Comninou, M. (1983) Energy relations for SH waves interacting with a frictional contact interface. *International Journal of Solids and Structures* **19,** 579–586.

Comninou, M., Barber, J. R. and Dundurs, J. (1982) Disturbance at a frictional interface caused by a plane elastic pulse. *Journal of Applied Mechanics* **49,** 361–365.

Comninou, M. and Dundurs, J. (1977a) Reflection from a rigid boundary involving separation. *Journal of Engineering Mechanics Division Proceedings ASCE* **103,** 285–294.

Comninou, M. and Dundurs, J. (1977b) Reflection and refraction of elastic waves in presence of separation. *Proceedings of the Royal Society of London Series A* **356,** 509–528.

Comninou, M. and Dundurs, J. (1977c) Elastic interface waves involving separation. *Journal of Applied Mechanics* **44,** 222–226.

Comninou, M. and Dundurs, J. (1978a) Singular reflection and refraction of elastic waves due to separation. *Journal of Applied Mechanics* **45,** 548–552.

Comninou, M. and Dundurs, J. (1978b) Elastic interface waves and sliding between two solids. *Journal of Applied Mechanics* **45,** 325–330.

Comninou, M. and Dundurs, J. (1979a) Interaction of elastic waves with a unilateral interface. *Proceedings of the Royal Society of London Series A* **368,** 141–154.

Comninou, M. and Dundurs, J. (1979b) Interface separation in the transonic range caused by a plane stress pulse. *Journal of Sound Vibration* **62,** 317–325.

Comninou, M. and Dundurs, J. (1980) Interface slip caused by an SH pulse. *International Journal of Solids and Structures* **16,** 283–289.

Comninou, M., Dundurs, J. and Chez, E. L. (1979) Total reflection of SH waves in presence of slip and friction. *Journal of Acoustic Society of America* **66,** 789–793.

Dundurs, J. and Comninou, M. (1979) Interface separation caused by a plane elastic wave of arbitrary form. *Wave Motion* **1,** 17–23.

Iwan, W. D. (1973) A generalization of the concept of equivalent linearization. *International Journal of Non-Linear Mechanics* **8,** 279–287.

Kern, G. A. and Kern, T. M. (1974) *Handbook of Mathematics.* McGraw-Hill, New York.

Miller, R. K. (1977) An approximate method of analysis of the transmission of elastic waves through a friction boundary. *Journal of Applied Mechanics* **44,** 652–656.

Miller, R. K. (1978) The effects of boundary friction on the propagation of elastic waves. *Bulletin of the Seismology Society of America* **68,** 987–998.

Miller, R. K. (1979) An estimate of the properties of Love-type surface waves in a frictionally bonded layer. *Bulletin of the Seismology Society of America* **69,** 305–317.

Miller, R. K. and Tran, H. T. (1979) Reflection, refraction and absorption of elastic waves at a frictional interface: SH motion. *Journal of Applied Mechanics* **46,** 625–630.

Miller, R. K. and Tran, H. T. (1981) Reflection, refraction and absorption of elastic waves at a frictional interface: P and SV motion. *Journal of Applied Mechanics* **48,** 155–160.

Wang, Y. S., Yu, G. L. and Gai, B. Z. (1997) Slip with friction between an elastic layer and a substrate caused by an SH pulse. *Mechanics Research Communications* **24,** 85–91.

Zharii, O. Y. (1995) Adhesive contact between the surface wave and a rigid strip. *Journal of Applied Mechanics* **62,** 368–371.

Zharii, O. Y. (1996) Frictional contact between the surface wave and a rigid strip. *Journal of Applied Mechanics* **63,** 15–20.

APPENDIX

The unit vectors defining the directions of motion and propagation of different waves follow from Fig. 1.

Incident SH wave: $n = 0$, $c_0 = c_T$

$$\mathbf{d}^{(0)} = (0, 0, 1), \quad \mathbf{p}^{(0)} = (\sin\theta_0, \cos\theta_0, 0). \tag{A1}$$

Reflected SH wave: $n = 2'$, $c_{2'} = c_T$

$$\mathbf{d}^{(2')} = (0, 0, 1), \quad \mathbf{p}^{(2')} = (\sin\theta_{2'}, -\cos\theta_{2'}, 0). \tag{A2}$$

Refracted SH wave: $n = 4'$, $c_{4'} = \bar{c}_T$

$$\mathbf{d}^{(4')} = (0, 0, 1), \quad \mathbf{p}^{(4')} = (\sin\theta_{4'}, \cos\theta_{4'}, 0). \tag{A3}$$

Induced P wave in the lower half space: $n = 1$, $c_1 = c_L$

$$\mathbf{d}^{(1)} = \mathbf{p}^{(1)} = (\sin\theta_1, -\cos\theta_1, 0). \tag{A4}$$

Induced SV wave in the lower half space: $n = 2$, $c_2 = c_T$

$$\mathbf{d}^{(2)} = (\cos\theta_2, \sin\theta_2, 0), \quad \mathbf{p}^{(2)} = (\sin\theta_2, -\cos\theta_2, 0). \tag{A5}$$

Induced P wave in the upper half space: $n = 3$, $c_3 = \bar{c}_L$

$$\mathbf{d}^{(3)} = \mathbf{p}^{(3)} = (\sin\theta_3, \cos\theta_3, 0). \tag{A6}$$

Induced SV wave in the upper half space: $n = 4$, $c_4 = \bar{c}_T$

$$\mathbf{d}^{(4)} = (-\cos\theta_4, \sin\theta_4, 0), \quad \mathbf{p}^{(4)} = (\sin\theta_4, \cos\theta_4, 0). \tag{A7}$$